Journal of Applied Electrochemistry **33**: 693–701, 2003.

Anodic oxidation of 2,4-dihydroxybenzoic acid for wastewater treatment

R.H. de LIMA LEITE, P. COGNET*, A.-M. WILHELM and H. DELMAS
Laboratoire de Génie Chimique; UMR 5503 CNRS/INPT/UPS/Site Basso-Cambo-srue Paulin Talabot 31106 Toulouse Cedex 01
*(*author for correspondence, fax: +33 5 61 55 78 95, e-mail: Patrick.Cognet@ensiacet.fr)*

Received 3 December 2001; accepted in revised form 6 March 2003

Key words: adsorption, 2,4-dihydroxybenzoic acid, electrochemistry, electrolysis, environment, pollution

Abstract

Dihydroxybenzoic acid (2,4-DHBA) is used as an intermediate chemical reactant in industrial synthetic processes. Disinfection of water contaminated by 2,4-DHBA, using chlorinating techniques, generates trihalomethane compounds, so that alternative degradation techniques are of interest. The electrochemical oxidation of 2,4-dihydroxybenzoic acid (2,4-DHBA) at a platinized titanium electrode was investigated. An electroanalytical study by linear and cyclic voltammetry showed adsorption of the reagent at the electrode surface. Mathematical treatment of cyclic voltammetry curves indicates Langmuir type adsorption. For electrolysis, working in the oxygen evolution region causes an increase in electroactive electrode surface area and better mass transfer at the electrode. For example, for an initial 2,4-DHBA concentration of 0.3 kg m^{-3} and a current density of 300 A m^{-2}, almost complete conversion of the pollutant is obtained after passing 4 A h, together with a TOC decrease of 30%. Byproducts of electrodegradation include 2,3,4- and 2,4,5-trihydroxybenzoic acids (THBA), maleic acid, glyoxalic acid and oxalic acid. The faradaic yield is less than 18%, due to oxygen evolution during electrolysis.

List of symbols

A	electrode surface area (m^2)
C_i	concentration of species i (mol m^{-3})
E_a	anodic potential (V vs SCE)
E_0'	normal apparent potential of the working electrode (V vs SCE)
E_{peak}	peak potential (V vs SCE)
F	faradaic constant (96 487 C mol^{-1}) (C mol^{-1})
I	current (A)
i	current density (A m^{-2})
I_{peak}	current peak (A)
I_{peak}^{sat}	current peak for the saturated electrode surface (A)
$k°$	standard heterogeneous rate constant (m s^{-1})
k_d	mass transfer coefficient (m s^{-1})
n	total number of electrons exchanged in the electrochemical process
n_a	number of electrons exchanged in the limiting electron transfer step
Q_i	electricity amount necessary to form one mole of compound i (C)
R	gas molar constant (8.314 J mol^{-1} K^{-1})
S_{el}	electrode active surface area (m^2)
T	temperature (°C)
t	time (s)
v	potential scan rate (V s^{-1})
V	volume of solution (m^3)
$\dot{V}_G$	gas flow rate (m^3 s^{-1})

Greek symbols

α	charge transfer coefficient (–)
θ	covering level (–)
Γ_0^*	initial surface concentration (mol m^{-2})
Γ_i	surface concentration of species i (mol m^{-2})
β_i	adsorption coefficient of species i (m^3 mol^{-1})
v_i	stoichiometric coefficient of species i (–)
Γ_s	saturation surface concentration (mol m^{-2})

1. Introduction

The elimination of toxic organic compounds in industrial wastewater is a difficult problem, because each pollutant requires a specific treatment. Biological treatment is the most frequently used method for wastewater clean-up because of its low cost. However, it is not always an appropriate method in the presence of recalcitrant biological organic pollutants. For example, some organics, like phenols, inhibit bacterial growth making biological effluent purification impossible. In these cases, an alternative treatment is necessary. There are several chemical oxidation processes for organic pollutant destruction in liquid effluents. Wet air oxidation

[1–4], incineration [5] or ozone processes [6, 7] are often used. However, there is no universal method and reductions in levels of water contaminants as determined by environmental laws requires new processes [5]. Electrochemical oxidation is a promising alternative for organic pollutant removal in aqueous media.

Several papers show the possibility of eliminating organic compounds such as phenol [8], bisphenol [9], dyes [10], benzoic acid [11], chlorinated compounds [11], by electrooxidation processes. The indirect electrooxidation of phenol by electrogenerated hypochlorite at a Ti/IrO_2 anode proved to be particularly efficient since no chlorinated phenols were detected after electrolysis [8].

For experiments described in this article, platinized titanium was chosen as the anode material because the aim of this work was to study the influence of ultrasound irradiation on the electrochemical process [12]. Using electrocatalytic electrodes would not have allowed electrode and ultrasound activation effects to be separated.

In aqueous solutions, electrooxidation of an organic molecule proceeds through indirect electronic transfer between the organic compound and the platinum (Pt) anode. Oxygen atoms are transferred from the water molecule discharge at one electron leading to the formation of adsorbed hydroxyl radicals. The first step in this transfer process consists in the formation of adsorbed radical species such as $O^{\bullet}$, $HOO^{\bullet}$, $HO^{\bullet}$. Then, these very reactive radicals oxidize organic molecules [13–16]. According to Vitt and Johnson [17], the initial step in such a mechanism is the oxidation of water during the following reaction:

$$H_2O + PtO_x \rightarrow PtO_x[HO^{\bullet}] + H^+ + 1e^-$$

In the case of oxides having low oxygen evolution overvoltage, like PtO_x, Comninellis [18] suggests the following mechanism for anodic oxidation of organic molecules: physisorbed hydroxyl radicals react with the oxygen of PtO_x to form platinum at a higher oxidation state PtO_{x+1}. Finally, higher oxide sites PtO_{x+1} oxidize adsorbed organic molecules $PtO_x[R]$, regenerating the PtO_x sites according to

$$PtO_{x+1} + PtO_x[R] \longrightarrow 2\,PtO_x + RO$$

The suggested mechanism is shown in Figure 1.

The (mono-, di-, tri-, poly-) hydroxybenzoic acids may be regarded as kinds of simple model compounds for humic substances, because of their chemical structures. These acids, like humic substances, may form trihalomethane compounds. This is particularly relevant since hydroxybenzoic acids are used as intermediate chemicals in industrial synthetic processes [19, 20].

The electrooxidation of 2,4-dihydroxybenzoic acid (2,4-DHBA) was studied at a platinized titanium electrode. An electroanalytical study was first carried out to characterize the electrochemical behaviour of 2,4-DHBA. Then electrolysis parameters such as electrode potential or current density were investigated. Attention was also paid to the degradation product distribution. Finally, the faradaic yield was calculated.

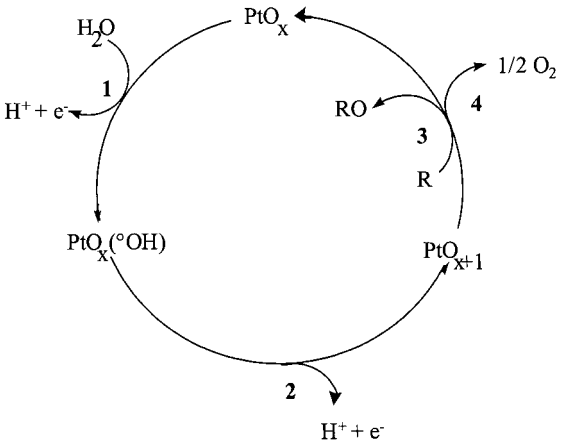

Fig. 1. Anodic oxidation mechanism. (1) Water electrooxidation; (2) higher oxide formation; (3) oxidation of organic molecules; (4) oxygen evolution.

2. Experimental methods

2.1. *Materials and reagents*

All chemicals were of highest purity (Fluka) and used as received. Only 2,4,5-trihydroxybenzoic acid was synthesized according to the procedure described elsewhere [21]. A mixture of 2,4,5-trihydroxybenzoic acid (88%) and 2,3,4-trihydroxybenzoic acid (12%) was then obtained and later used for standardization.

2.2. *Electrochemical analysis*

Voltammetric measurements of 2,4-dihydroxybenzoic acid (1 mol m^{-3}) in aqueous sodium sulfate solution (100 mol m^{-3}) were performed in a 10^{-4} m^3 thermostated electrochemical cell. The solution pH was adjusted to 2.0 with sulphuric acid and remained constant during electroanalysis. Water was treated by a Millipore ultrafiltration system (Milli-Q) and its resistivity measured at 0.18 MΩ m. The working electrode (anode) was a rotating platinum disc electrode with 3.14×10^{-6} m^2 of exposed surface. The counter electrode was a platinized titanium plate (5×10^{-4} m^2) and a saturated calomel electrode (SCE) was used as a reference, connected to the electrolytic cell by an agar–agar bridge. Solutions were degassed with argon for 20 min before each experiment. A Tacussel potentiostat/galvanostat PJT 35-2 was used, driven by a pilot.

For classical I/E curve recording, electrode rotation speed was fixed at 33.33 s^{-1}, which is an average value, satisfactory for obtaining a laminar flow hydrodynamic behaviour. For cyclic voltammetry, the electrode was stationary.

2.3. *Electrolysis apparatus*

The experimental set up used for electrooxidation of 2,4-DHBA consisted of a cylindrical glass vessel (total volume 5×10^{-4} m^3), mechanically stirred and thermostated by circulating a water/ethylene glycol mixture in the reactor jacket. It was mechanically stirred and the stirring rate was fixed at 8 s^{-1}.

Anode and cathode consisted of two discs made of expanded platinized titanium grids of microlink F provided by MagnetoChemie, having a link coefficient (active surface area/geometrical surface area) of 2.2. Each electrode had a 52.2×10^{-4} m^2 geometrical surface area. The electrolysis cell was not divided. For potentiostatic experiments, a saturated calomel electrode was used as a reference, connected to the electrolytic cell by an agar–agar bridge. All experiments were performed at a temperature of 30 ± 3 °C. For galvanostatic electrolyses, constant current was supplied by the previously mentioned potentiostat/galvanostat. The electrolytic solution was the same as for the electroanalytical tests (Na_2SO_4 100 mol m^{-3} and pH 2.0), but the 2,4-DHBA concentrations employed were 0.1 or 0.3 kg m^{-3}. The value of pH 2 was arbitrarily chosen because the results of this study were to be compared with those obtained by sonooxidation alone [22]. For the latter case, pH values of 2, 7, 12 were tested. It appeared that working at pH 2 did not require monitoring of the pH during sonooxidation experiments [22], which was not the case for pH values of 7 or 12.

2.4. *Product analysis*

Samples were analysed using an HPLC (Merck L-6200A intelligent pump) equipped with an array diode detector (Merck L-3000). Absorption u.v. spectra were registered each 2.5 s elution time. The aromatic compound analysis was monitored using the following conditions: RP-18 reversed phase Merck column, 0.25 m length, 5×10^{-6} m particle size; two mobile phases, A and B (A, water/acetonitrile/THF: 90/5/5; B, water/acetonitrile/THF: 65/30/5), were used for an elution gradient (gradient of solution A: 100% 0–300 s, variation of 100 to 90% 300–600 s, 90 to 0% 600–1200 s, and 0% 1200–1800 s), at a flow rate of 1.17×10^{-8} m^3 s^{-1}. For aromatic compounds, absorbance was measured at 260 nm.

Nonaromatic products were separated using a Polyspher® OA KC Merck column and a H_2SO_4 0.005 N solution as mobile phase with a flow rate of 5×10^{-9} m^3 s^{-1}. External calibration was carried out in order to estimate the concentrations of each aliphatic product from peak area measurements at 210 nm, for each series of experiments. To identify 2,4-DHBA degradation byproducts, elution times and u.v. spectra of peaks obtained for byproducts of 2,4-DHBA degradation were compared to those of pure reagents.

The total organic carbon (TOC) was measured with a Shimadzu TOC analyser. Samples were first acidified and dissolved CO_2 was eliminated by air bubbling before injection. TOC was calculated from the standardization curve obtained with solutions of known TOC.

3. Results and discussion

3.1. *Electroanalytical study*

3.1.1. *Linear sweep voltammetry*

For this study, the disc electrode was rotated so that 2,4-DHBA was 'pumped' from the bulk solution to the vicinity of the electrode surface and was continuously regenerated. Under mechanical stirring, the current/potential curve shows only one peak with $E_{1/2}$ value = 1.02 V vs SCE and a shape suggesting blocking phenomena possibly due to polymer formation: the current drops instead of remaining constant. The polymerization of the organic pollutant is a side reaction in 2,4-DHBA electrooxidation, and has been observed for other electrooxidation reactions of aromatics, such as phenol on a platinum electrode. Comninellis [19] has studied the electrodegradation of phenol at a platinized titanium electrode and has observed the appearance of a dark yellow film, insoluble in acetone. The presence of such a film is favoured by a basic pH, a current density below 30 mA cm^{-2} and a temperature above 50 °C [8]. In this case, phenol is initially oxidized to a phenoxy radical, which can in turn either be transformed into quinone or dimerize [23]. The so formed dimers are further oxidized into radicals at a lower potential than phenol itself. The polymer chain can then be propagated by addition of new phenol units.

3.1.2. *Cyclic voltammetry*

High potential scan rates were used and the electrolytic cell was not stirred (fixed electrode) so that 2,4-DHBA was transferred from the bulk solution to the electrode only by diffusion. The potential scan rate was varied between 0.1 and 1 V s^{-1}. The potential was varied from −0.3 to 1.5 V vs SCE.

A reference voltammogram was initially recorded using a 100 mol m^{-3} Na_2SO_4 solution at pH 2 adjusted with sulfuric acid. Oxygen evolution occurs at around 1.25 V vs SCE. Pt oxidation was not observed since it occurs in the oxygen evolution zone. A cathodic peak was observed at 0.27 V vs SCE, which corresponds to the reduction of platinum oxides PtO_x [23].

Figure 2 shows cyclic voltammograms recorded using a 10 mol m^{-3} 2,4-DHBA solution at different scan rates. An oxidation peak is observed at 1.1 V vs SCE and no cathodic reverse peak is associated, the single cathodic peak corresponding to the reduction of PtO_x. This shows that the 2,4-DHBA electrooxidation process is irreversible. Voltammograms were recorded at different potential scan rates. No post- or prepeak is observed, suggesting that only the adsorbed 2,4-DHBA is electroactive. In the case of an irreversible electrochemical

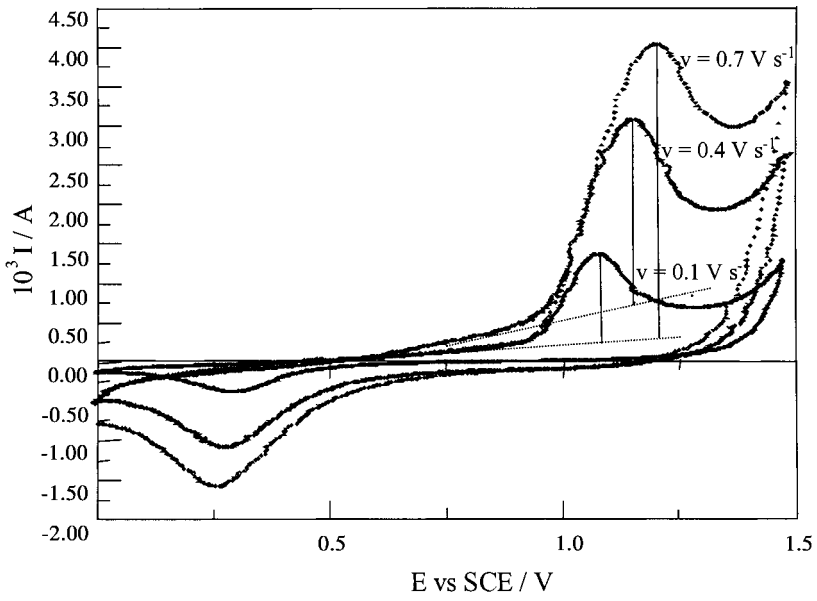

Fig. 2. Cyclic voltammograms of a 2,4-DHBA solution (10 mol m^{-3} 2,4-DHBA, 100 mol m^{-3} Na_2SO_4 solution (pH 2 adjusted with H_2SO_4) at a platinum disc electrode (dia. 2×10^{-3} m), recorded at different potential scan rates.

reaction of an adsorbed species, the oxidation current peak can be expressed [24]:

$$I_{\text{peak}} = \frac{n\alpha n_a F^2 A v \Gamma_0^*}{2.718\ RT} \tag{1}$$

where n is the total number of electrons exchanged in the electrochemical process, α the charge transfer coefficient, n_a, the number of electrons exchanged in the limiting electron transfer step, A the electrode surface area, v the potential scan rate and Γ_0^*, the initial 2,4-DHBA surface concentration.

The potential of the oxidation peak is given by [24]:

$$E_{\text{peak}} = E^{\circ\prime} + \frac{RT}{\alpha n_a F} \ln\left(\frac{RT}{\alpha n_a F} \times \frac{k^\circ}{v}\right) \tag{2}$$

where $E^{\circ\prime}$ is the normal apparent potential of the working electrode and k° the standard heterogeneous rate constant.

Increasing the potential scan rate results in a shift of the oxidation potential peak towards more anodic potentials. Figure 3 shows a linear variation of the peak potential with ln v, confirming that the electrochemical system is irreversible. Figure 4 shows that the oxidation peak current varies linearly with the potential scan rate, indicating adsorption of 2,4-DHBA at the electrode surface [24].

3.1.3. *Adsorption isotherm*

Voltammograms of 2,4-DHBA at a concentration of 0.385 kg m^{-3} were first recorded for different electrode immersion times (from 20 s to 10 min). All were identical, showing that adsorption of 2,4-DHBA was a fast process.

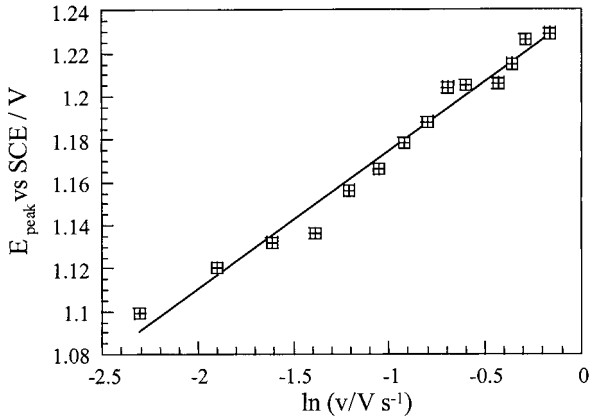

Fig. 3. Variation of the anodic peak potential against ln v for the oxidation of 2,4-DHBA (10 mol m^{-3}) on platinum.

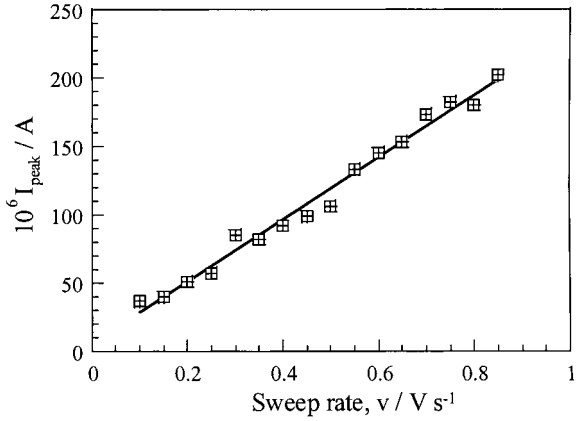

Fig. 4. Variation of the anodic peak current against v for the oxidation of 2,4-DHBA (10 mol m^{-3}) on platinum.

Gattrell and Kirk [23] have shown that phenol is strongly adsorbed on platinum: the oxidation wave was

observed even after rinsing of the electrode and immersion in supporting electrolyte for 300 s. This phenomenon was not observed in the case of 2,4-DHBA: no oxidation wave was detected after applying the same treatment to the electrode, proof of rapid desorption.

Cyclic voltammograms obtained for different concentrations of 2,4-DHBA can be used to establish a relation between the 2,4-DHBA surface concentration Γ and its bulk concentration C, the adsorption equilibrium curve.

For a given potential scan rate and at a constant temperature, I_{peak} is proportional to Γ_0^* and assuming that equilibrium of the electrode is rapidly attained, Γ_0^* is equal to $\Gamma_{2,4\text{-DHBA}}$. In the same way, I_{peak}^{sat} corresponds to saturation of the electrode surface. Voltammograms obtained at 25 °C and for different 2,4-DHBA concentrations are shown in Figure 5. The shape of the equilibrium curve indicates that the adsorption can be described with a Langmuir isotherm, whose equation can be expressed as [24]:

$$\Gamma_{DHBA} = \frac{\Gamma_S \beta_{DHBA} C_{DHBA}}{1 + \beta_{DHBA} C_{DHBA}} \quad (3)$$

where Γ_S is the saturation surface concentration and $\beta_{2,4\text{-DHBA}}$, the adsorption coefficient of 2,4-DHBA. Values of $\beta_{2,4\text{-DHBA}}$ and I_{peak}^{sat} were determined by nonlinear regression of the experimental points I_{peak} vs $C_{2,4\text{-DHBA}}$ and are respectively equal to 1187×10^{-6} A and 301.27×10^{-3} m^3 mol^{-1}. Figure 6 shows the agreement between model and experimental results.

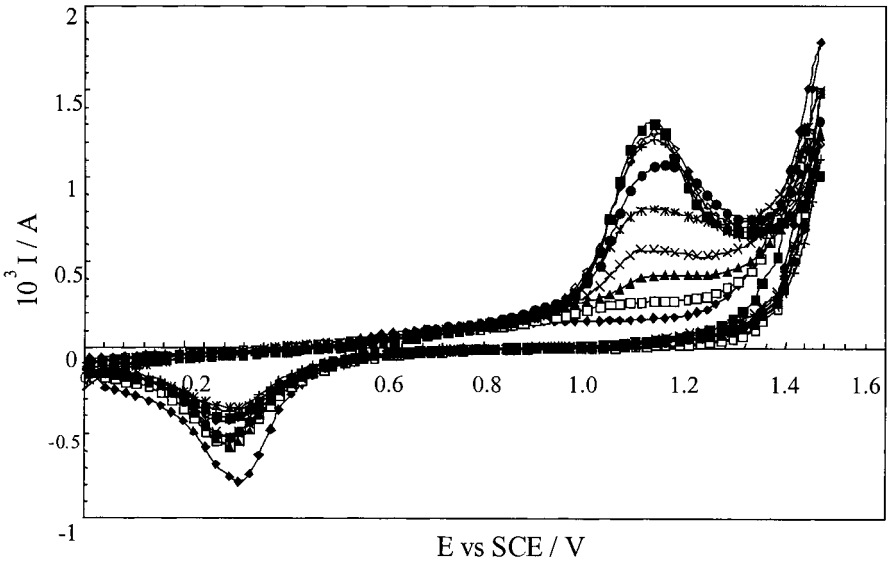

Fig. 5. Cyclic voltammograms obtained for different 2,4-DHBA concentrations (100 mol m^{-3} Na_2SO_4 solution, pH 2 adjusted with H_2SO_4) at a platinum disc electrode (dia. 2×10^{-3} m), scan rate: 0.1 V s^{-1}. Concentration: (♦) 0, (□) 0.1, (▲) 0.5, (×) 1.0, (✳) 2.5, (●) 5.0, (+) 7.5, (◊) 10, (■) 25 mol m^{-3}.

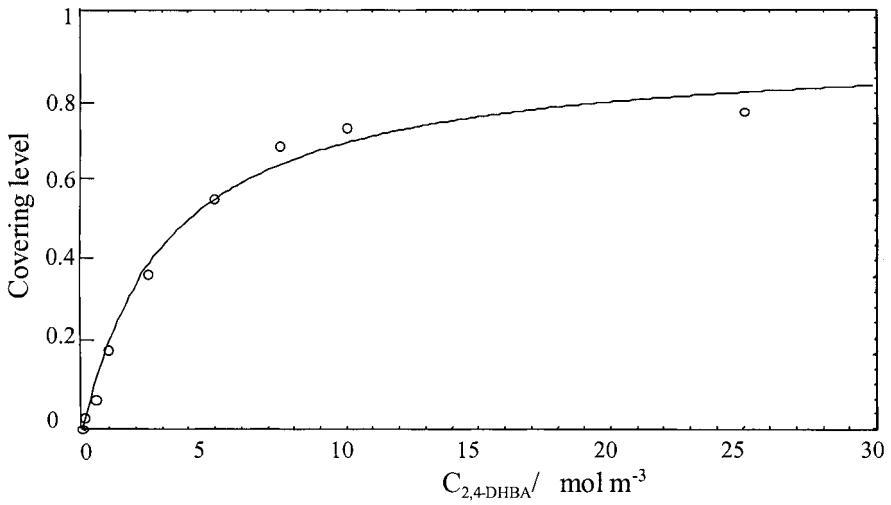

Fig. 6. Covering rate as a function of 2,4-DHBA concentration, experimental data and model.

3.2. *Electrolysis performance*

3.2.1. *Potentiostatic electrolysis*

The working electrode potential is a key parameter since it governs the product distribution of the degradation process. The choice of the working potential was determined by the rate of oxygen production: at 1.2 V vs SCE, oxygen evolution does not occur, 1.5 V vs SCE corresponds to weak oxygen evolution and at 2.0 V vs SCE, oxygen evolution is high. Current curves during potentiostatic operation are shown in Figure 7 while Figure 8 shows the variation of 2,4-DHBA concentration during electrolysis for each potential.

For a 1.2 V vs SCE working electrode potential, current decreases from around 3 to 1.5×10^{-3} A ($t = 1200$ s) and only 10% of 2,4-DHBA is converted at $t = 10\,800$ s. Current drop, the ratio $I_{t=1200\ s}/I_{t=0\ s}$, can be interpreted in terms of electrode passivation by a polymer film and it corroborates the conclusions from analysis. As the electrode is passivated, electrooxidation of 2,4-DHBA slows, resulting in poor conversion. Final conversion is much better when working at a 1.5 V vs SCE (35% for $t = 10\,800$ s) and current drop is reduced but is still equal to 50%. At this potential, current is due to 2,4-DHBA electrooxidation but also to oxygen evolution. Presumably, the latter partly destroys the organic film which covers the electrode and accelerates mass transfer by turbulence. Finally, working at a 2.0 V vs SCE results in intense oxygen evolution. At the potential used, oxygen evolution does not lead to the formation of a bubble curtain. Moreover, the working electrode is made of expanded metal and is placed above the counter electrode, which means that oxygen bubbles can easily escape from the electrode surface, avoiding the formation of a curtain. The contribution of 2,4-DHBA oxidation to the overall current becomes negligible: current is almost entirely due to water oxidation and remains constant. Rapid conversion of 2,4-DHBA is obtained; total conversion is obtained after 3000 s. Since dissolved oxygen does not oxidize 2,4-DHBA, enhancement of the conversion rate with increasing applied potential can only be attributed to greater electrode activity.

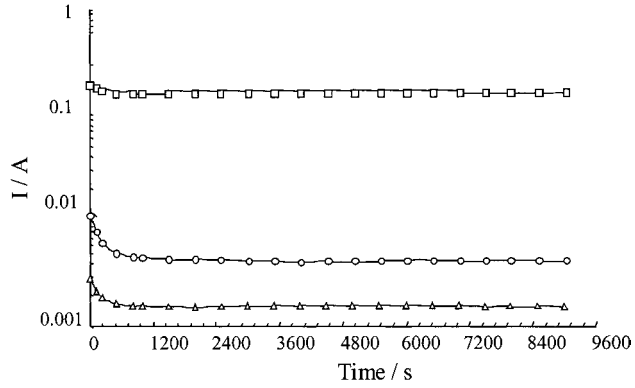

Fig. 7. Current variation for a potentiostatic electrolysis. Temperature 27 °C; initial 2,4-DHBA concentration 0.1 kg m^{-3}; volume of the solution 2×10^{-4} m^3. Key: (△) 1.2, (○) 1.5 and (□) 2.0 V vs SCE.

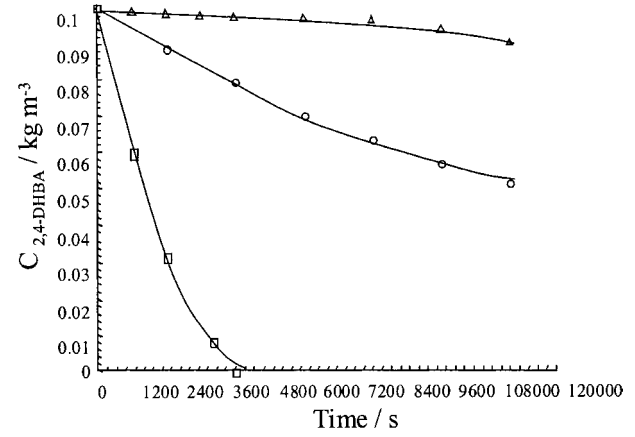

Fig. 8. Variation of the 2,4-DHBA concentration with time for constant potential electrolyses. Temperature 27 °C; initial 2,4-DHBA concentration 0.1 kg m^{-3}; volume of the solution 2×10^{-4} m^3. Key: (△) 1.2, (○) 1.5 and (□) 2.0 V vs SCE.

It is well-known that the mass transfer coefficient between electrolyte and electrode increases when gas bubbles are electrogenerated at an electrode surface, especially during the growth and the separation of bubbles. The mass transfer coefficient can be expressed as

$$k_d = a\left(\frac{\dot{V}_G}{S_{el}}\right)^b \tag{4}$$

where S_{el} is the electrode active surface area, which may be different from A in the case of passivation phenomena, $\dot{V}_G$ is the oxygen flow rate, a depends on experimental conditions and b is close to 0.5 [25]. For a mass transfer limited electrochemical process, the current of 2,4-DHBA electrooxidation can be expressed as $I = n\,F\,S_{el}\,k_d\,C_{2,4\text{-DHBA}}$.

Thus, the better conversion rate obtained at a higher electrode potential, which causes a higher oxygen evolution, is due either to mass transfer enhancement or to electrode surface enhancement. In the specific case of 2,4-DHBA electrooxidation, oxygen evolution helps to depassivate the electrode. Thus, increasing oxygen evolution, which means increasing E, results in an increase in the electrode active surface area S_{el}. According to Equation 4, k_d depends on the ratio $\dot{V}_G/S_{el}$. As both $\dot{V}_G$ and S_{el} increase with increasing E, it is difficult to know if k_d really increases. Presumably, when increasing E, k_d might increase slightly until the electrode is entirely depassivated and then, it can be expected that S_{el} remains almost constant and that k_d increases with $\dot{V}_G$.

3.2.2. *Constant current electrolysis*

The influence of current density and other operating conditions on galvanostatic electrolysis performance were investigated. Current density is a parameter of

great importance for the oxidation of organic compounds [26, 27]. In the case of phenol electrooxidation, low current densities lead to surface passivation by polymer films. Using a larger current density leads to oxygen evolution, which can favour depassivation of the electrode but is detrimental to faradaic yield.

Two different anodic current densities were tested: 100 and 300 A m^{-2}. Results are shown in Figure 9. The amount of electricity necessary for a given conversion of 2,4-DHBA is reduced at the lower current density. For example, for a 90% conversion of 2,4-DHBA, it increases from 1 Ah for 100 A m^{-2} to 2 for 300 A m^{-2}. However, the time necessary for the operation is extended.

The effect of the initial 2,4-DHBA concentration was also investigated, using a 300 A m^{-2} current density.

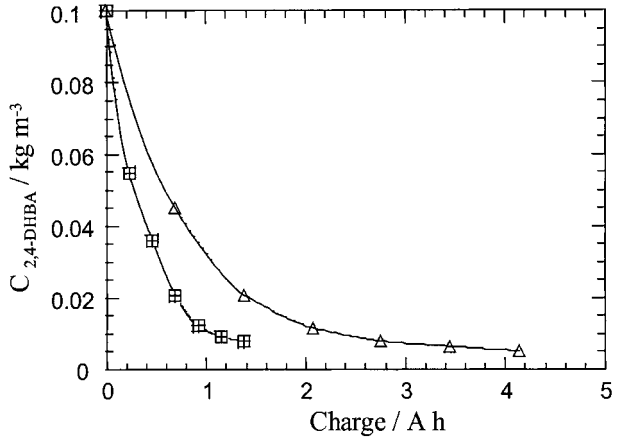

Fig. 9. Variation of the 2,4-DHBA concentration with the amount of consumed electricity for constant current electrolyses. Temperature 27 °C; initial 2,4-DHBA concentration 0.1 kg m^{-3}; volume of the solution 2×10^{-4} m^3. Key: (⊞) 100 and (△) 300 A m^{-2}.

Initial concentrations of 0.1 and 0.3 kg m^{-3} were tested. After passing 0.69 Ah, a 2,4-DHBA conversion of 58.6% was obtained in the first case, compared to 31.5% in the second, corresponding to 21 and 34×10^{-6} kg $(Ah)^{-1}$ of degraded 2,4-DHBA, respectively. The percentage conversion of 2,4-DHBA is lower at the higher initial concentration but the total amount of degraded 2,4-DHBA is increased. For example, a 84% conversion is obtained in 45 min for an initial concentration of 0.3 kg m^{-3} and a 300 A m^{-2} current density. It can be linked to results obtained by cyclic voltammetry which showed that the proportion of the electrode surface covered increases with 2,4-DHBA concentration thus accelerating the conversion rate. According to Figure 6, the initial covering level is 10% for 0.1 kg m^{-3} and 20% for 0.3 kg m^{-3} 2,4-DHBA initial concentration.

(a) *Product distribution*. Initially, the major degradation products were separated and identified by HPLC. Aromatic compounds produced during 2,4-DHBA electrodegradation were 2,3,4- and 2,4,5-trihydroxybenzoic acids (THBA), both hydroxylated derivatives of the 2,4-DHBA. The short chain aliphatic acids identified were maleic acid, glyoxalic acid and oxalic acid. Other products were detected by HPLC but could not be identified. A decrease in the total organic carbon (TOC) value was also observed and attributed to CO_2 formation.

Figures 10 and 11 show the concentration profiles of 2,4-DHBA and byproducts. CO_2 was estimated by difference: % $CO_2 = 100 \times (\text{initial } TOC_{t=0} - TOC_t)/TOC_{t=0}$. There is a significant loss in the TOC balance (around 20%), which can be attributed to the formation of unidentified compounds. The current density was 300 A m^{-2} in all cases. Only a small amount of hydroxylated products is formed by electrooxidation,

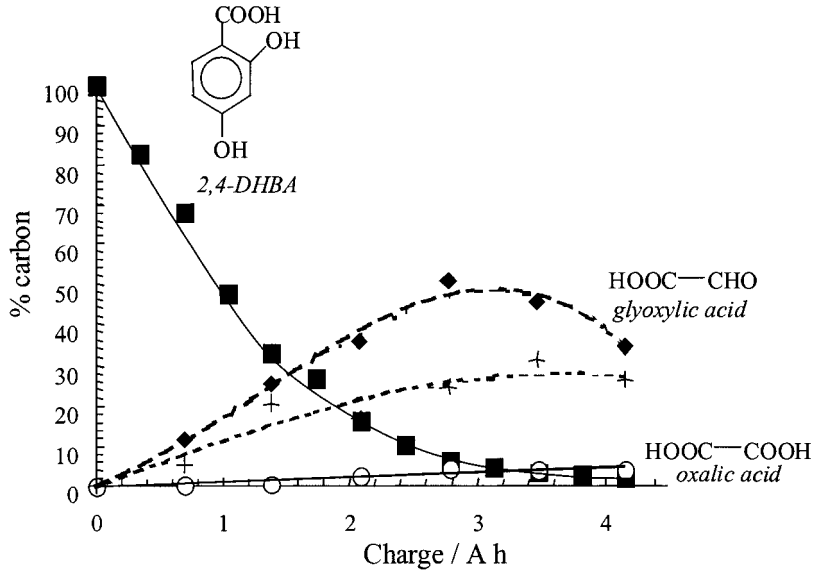

Fig. 10. Variation of the concentrations (expressed as a percentage of the total carbon) of 2,4-DHBA and of the main byproducts formed during 2,4-DHBA electrooxidation. Temperature 30 °C; initial 2,4-DHBA concentration 0.3 kg m^{-3}; volume of the solution 2×10^{-4} m^3; current density 300 A m^{-2}. Key: (■) 2,4-DHBA; (♦) glyoxylic acid; (○) oxalic acid; (+) CO_2.

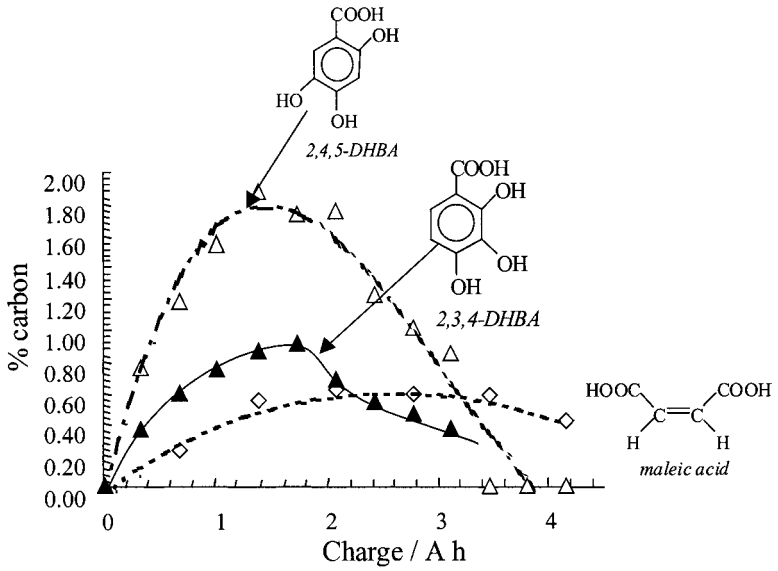

Fig. 11. Variation of the concentrations (expressed as a percentage of the total carbon) of minor byproducts formed during 2,4-DHBA electrooxidation. Temperature 30 °C; initial 2,4-DHBA concentration 0.3 kg m^{-3}; volume of the solution 2×10^{-4} m^3; current density 300 A m^{-2}. Key: (▲) 2,3,4-THBA; (△) 2,4,5-THBA; (◊) maleic acid.

compared with [22]. Studies of the electrooxidation of other aromatic molecules, such as phenol, have shown that the reaction path leads to the formation of non-negligible amounts of intermediate hydroxylated species such as hydroquinone and catechol [10, 23, 28]. Two hypotheses can be formulated to explain the lower amount of hydroxylated products formed during the electrooxidation of 2,4-DHBA: either hydroxylated products are formed but undergo consecutive rapid oxidation steps before desorption from the electrode surface or the reaction path is different from that observed for phenol electrooxidation and would lead to early breakage of the cycle.

Marquier [29] has studied the degradation of 2,4-DHBA by photocatalysis on titanium oxide. He has shown that no aromatic intermediate product was formed, the only byproducts identified being glyoxalic and oxalic acids. It seems that 2,4-DHBA reacts directly with holes, h^+, at the TiO_2 surface and the authors propose a reaction path involving the opening of the ring at an early stage of the reaction. According to Figure 10, 2,4-DHBA electrodegradation obeys a consecutive-competitive scheme. The main pathway consists in the degradation of 2,4-DHBA into glyoxylic acid and this intermediate product is further oxidized into CO_2 and oxalic acid, suggesting the early opening of the ring.

(b) *Faradaic yield.* The overall faradaic yield for the electrooxidation of 2,4-DHBA was calculated from concentrations of intermediate products and TOC, both monitored during the reaction. Calculations were made according to the following balanced equations:

$$\underset{\text{(2,4-DHBA)}}{C_7H_6O_4} + H_2O \rightarrow \underset{\text{(2,3,4- or 2,4,5-THBA)}}{C_7H_6O_5} + 2\,H + + 2\,e^-$$

$$C_7H_6O_4 + 6\,H_2O \rightarrow \underset{\text{maleic acid}}{C_4H_4O_4} + 3\,CO_2 + 14\,H^+ + 14\,e^-$$

$$C_7H_6O_4 + 7\,H_2O \rightarrow 3\,\underset{\text{glyoxalic acid}}{C_2H_2O_3} + CO_2 + 14\,H^+ + 14\,e^-$$

$$C_7H_6O_4 + 10\,H_2O \rightarrow 3\,\underset{\text{oxalic acid}}{C_2H_2O_4} + CO_2 + 20\,H^+ + 20\,e^-$$

$$C_7H_6O_4 + 10\,H_2O \rightarrow 7\,CO_2 + 26\,H^+ + 26\,e^-$$

The charge Q_i, necessary to produce one mole of compound i from 2,4-DHBA can be calculated from the following equation:

$$Q_i = n_i F \frac{C_i}{\nu_i} V \tag{5}$$

The overall CO_2 concentration $(CO_2)_t$ was calculated from TOC data, by difference, then the concentration of CO_2 which was not produced together with maleic acid, glyoxylic acid or oxalic acid, (CO_2), was calculated by

$$(CO_2) = (CO_2)_t - 3\,(C_4H_4O_4) - 1/3\,(C_2H_2O_3) - 1/3\,(C_2H_2O_4) \tag{6}$$

and Q_{CO_2} obtained from

$$Q_{CO_2} = \frac{26F(CO_2)V}{7} \tag{7}$$

The overall charge Q_{total} used for 2,4-DHBA degradation is given by

$$Q_{\text{total}} = \sum_i Q_i = FV \sum_i n_i \frac{C_i}{\nu_i} \tag{8}$$

Finally, the overall faradaic yield is given by

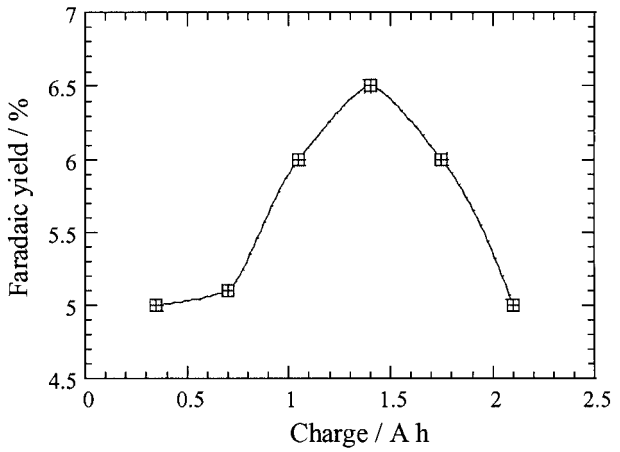

Fig. 12. Variation of the faradaic yield calculated from data related to Figures 10 and 11.

$$R_f\% = \frac{Q_{total}}{It} \quad (9)$$

Figure 12 shows the variation in the faradaic yield during the electrooxidation at 300 A m^{-2}. Faradaic yield remains below 7%, because of the high rate of the oxygen evolution. The faradaic yield seems to slightly increase during the electrooxidation and then diminish. This small decrease in the faradaic yield could be attributed to the poor electrochemical activity of glyoxalic and oxalic acids, which are formed at the end of the reaction.

4. Conclusions

Electroanalytical study has shown that 2,4-DHBA is an irreversible electroactive system involving adsorption phenomena and is therefore a good vehicle for investigating the efficiency of the electrochemical degradation technique. Working in the oxygen evolution zone enables the electrodes to be depassivated and the conversion rate to be increased. Moreover, intermediary products are mainly non-aromatic and can be further degraded to carbon dioxide as final product. Thus, the electrochemical technique proved to be an efficient and nonpolluting technique for the degradation of 2,4-DHBA. For example, a 84% conversion was obtained in 2700 s for an initial concentration of 0.3 kg m^{-3} and 300 A m^{-2}.

Among the modern techniques used in wastewater treatment, electrochemistry is promising because it only uses electrons as reactant and no recycling of chemical reagents is needed. It has been shown that it can be successfully applied to 2,4-DHBA degradation, where the electrochemical process is limited by electrode passivation and low pollutant concentrations.

References

1. J. Levec, *Chem. Biochem. Eng.* **11**(1) (1997) 47.
2. Q. Zhang and K.T. Chuang, *Ind. Eng. Chem. Res.* **37** (1998) 3343.
3. V. Tukac and J. Hanika, *Chem. Biochem. Eng. Q.* **11** (1997) 187.
4. V. Tukac and J. Hanika, *Chem. Biochem. Eng. Q.* **71** (1998) 262.
5. D.H. Belhatech, *Chem. Eng. Prog.* (Aug. 1995) 32.
6. J. Hoigné, *in* R.G. Rice and A. Netzer (Eds), 'Handbook of Ozone Technology and Applications', Vol. 1 (Butterworth, 1982).
7. J. Hoigné and H. Bader, *in* F.E. Brinckman and J.M. Bellama (Eds), 'Organometals and Organometalloids: Occurrence and Fate in the Environment', (American Chemical Society. Symposium Series, Washington, DC) **82** (1978) 292.
8. C. Comninellis and A.J. Nerini, *J. Appl. Electrochem.* **25** (1995) 23.
9. A.B. Boscoletto, F. Gottardi, L. Milan, P. Pannochia, V. Tartari, M. Tavan, R. Amadelli, A. De Battisti, A. Barbieri, D. Patracchini and G. Battaglin, *J. Appl. Electrochem.* **24** (1994) 1052.
10. S.M. McClung and A.T. Lemley, *Textile Chemistry of Colorist* **26** (1994) 17.
11. S. Stucki, R. Kötz, B. Carcer and W. Suter, *J. Appl. Electrochem.* **21** (1991) 99.
12. R.H. De Lima Leite, Thèse de doctorat, INPT Toulouse (1999).
13. H. Chang and D.C. Johnson, *J. Electrochem. Soc.* **136** (1989) 17.
14. B. Fleszar and D.B. Ploszynska, *Electrochim. Acta* **30** (1985) 31.
15. D. Wabner, and C.J. Grambow, *J. Electrochem. Soc.* **195** (1985) 95.
16. I.H. Yeo, S. Kim, R. Jacobson and D.C. Johnson, *J. Electrochem. Soc.* **136** (1989) 1395.
17. J.E. Vitt and D.C. Johnson, *J. Electrochem. Soc.* **139** (1992) 774.
18. C. Comninellis and G.P. Vercesi, *J. Appl. Electrochem.* **21** (1991) 335.
19. C. Comninellis and C. Pulgarin, *J. Appl. Electrochem.* **21** (1991) 703.
20. J.C. Catonné, 'Traitement des Effluents par Voie Electrochimique', *Galvano-Organo-Traitements de Surface* (Dec. 1993) 1073.
21. S. Rajagopalan, T.R. Seshadri and F.A. Varaderajan, 'A new synthesis of asaronic acid and aldehyde and their derivatives', *in* Proceedings of the Indian Academy of Science **A30** (1949) p. 265.
22. R.H. De Lima Leite, M-T. Maurette, A-M. Wilhelm and P.H. Delmas, 2nd European Congress of Chemical Engineering (ECCE 2), Montpellier (France) in *Récents progress en genie des procédés* **13** (1999) 17.
23. M. Gattrell and D.W. Kirk, *J. Electrochem. Soc.* **140** (1993) 903.
24. A.L. Bard and L.R. Faulkner, 'Electrochimie: Principes, Méthodes et Applications' (Masson, 1983), p. 791.
25. H. Vogt, *in* 'Comprehensive Treatise of Electrochemistry' (Plenum, 1983), Chapter 7, 445.
26. L. Chiang, J. Chang and T.J. Wen, *Environ. Sci. Health* **A30** (1995) 753.
27. G.A. Al-Enezi, H. Shaban and M.S.E. Abdo, *Desalination* **95** (1994) 1.
28. D.J. Walton and S.S. Phull, *Adv. Sonochem.* **4** (1996) 205.
29. F.B. Marquier, E.P. Costes, A.M. Braun, E. Oliveros and M-T. Maurette, *J. Photochem. Photobiol. A: Chemistry* **108** (1997) 65.